Downregulation of Connexin 43 Expression by High Glucose Reduces Gap Junction Activity in Microvascular Endothelial Cells

Tsuyoshi Sato, Robert Haimovici, Richard Kao, An-Fei Li, and Sayon Roy

Impairment of retinal vascular homeostasis is associated with the development and progression of diabetic retinopathy involving gap junction intercellular communication (GJIC) activity. The principal gap junction protein of intercellular communication, connexin, was investigated to determine the effects of high glucose concentrations on the expression of endothelial-specific connexins (Cx37, Cx40, and Cx43), connexin phosphorylation pattern, and GJIC activity. Rat microvascular endothelial (RME) cells grown in high (30 mmol/l)-glucose medium for 9 days had reduced Cx43 expression: Cx43 mRNA (68 ± 13% of control; $P = 0.019$, $n = 5$) and protein (55.6 ± 16% of control; $P = 0.003$, $n = 5$) levels were reduced; however, Cx37 and Cx40 expression was not affected. Using alkaline phosphatase and Western blot analyses, we identified three forms of Cx43: a nonphosphorylated form (P0) and two phosphorylated forms (P1 and P2). Expression of all three forms was decreased in cells grown in high-glucose medium: PO, 73 ± 15% of control ($P = 0.04$); P1, 57 ± 16% of control ($P = 0.01$); and P2, 42 ± 22% of control ($P = 0.006$). Using immunofluorescence microscopy, we observed Cx43 localization at specific sites of contact (plaques) between adjacent cells. In cells grown in high-glucose medium, we observed reduced plaque counts (63 ± 6% of control; $P = 0.009$) and decreased intensity of Cx43 immunofluorescence compared with cells grown in normal medium. Furthermore, using scrape load dye transfer (SLDT) technique, we found that these cells exhibited reduced GJIC activity (60% of control; $P = 0.01$, $n = 5$). The reduction in GJIC activity correlated with the decreased Cx43 protein levels ($r = 0.9$). These results indicate that high glucose concentrations inhibited GJIC activity by reducing Cx43 synthesis in RME cells. Impaired intercellular communication may contribute to breakdown of homeostatic balance in diabetic microangiopathy.
***Diabetes* 51:1565–1571, 2002**

Gap junctions are membrane channels that allow transfer of ions and small molecules between adjacent cells. Morphological studies using immunostaining show that gap junctions are composed of a family of proteins collectively called connexins (1). In most tissues, including retina, adjacent cells communicate through gap junctions involving connexins. In the retina, connexin 43 (Cx43) is abundantly present, which suggests a substantial amount of gap junctional coupling in the glial syncytium (2,3). In particular, endothelial cells and pericytes contain gap junctions and exhibit junctional transfer both in vitro (4) and in vivo (5). Morphometric analysis using electron microscopy of human retinal capillaries has shown that the basement membrane interposed between endothelial cell and pericyte is sufficiently thin to permit cell membrane contacts between these cells (6). Junctional transfer of molecules involving endothelin-1 between microvascular endothelial cells and pericytes has been reported to mediate endothelial cell–dependent proliferation of pericytes (7). Therefore, changes in gap junction intercellular communication (GJIC) activity may disrupt homeostasis between retinal vascular cells, leading to alterations in the blood-retinal barrier (BRB).

Chronic hyperglycemia in diabetes is associated with the development and progression of pathological changes in the retinal vasculature involving the breakdown of the BRB. The endothelium forms the BRB in the retinal capillary vessels, and its permeability is largely regulated by intercellular junctions (8,9). High-glucose conditions have been shown to reduce GJIC in RPE cells, which form the outer BRB (10). In Cx43-knockout mice, characteristic junctional contacts and the close apposition between lens epithelial cells are lost, leading to disturbed cellular organization and loss of structural integrity (11). These findings indicate that impaired GJIC among retinal vascular cells under high-glucose conditions may lead to structural failure and BRB breakdown.

Vascular endothelial cells express three types of connexin, Cx37, Cx40, and Cx43 (12), whose distribution within the vasculature (13) varies widely with the species studied. Two forms of cellular Cx43 have been reported, the nonphosphorylated and the phosphorylated high-molecular-weight form. However, the functional significance of these forms of Cx43 in GJIC activity is unclear. The nonphosphorylated Cx43 is believed to mediate GJIC

From the Department of Ophthalmology, Boston University School of Medicine, Boston, Massachusetts.

Address correspondence and reprint requests to Sayon Roy, Department of Ophthalmology, Boston University School of Medicine, 715 Albany St., Boston, MA 02118. E-mail: sayon@bu.edu.

Received for publication 28 November 2001 and accepted in revised form 18 January 2002.

AP, alkaline phosphatase; BRB, blood-retinal barrier; Cx, connexin; GJIC, gap junction intercellular communication; SLDT, scrape-loading dye transfer.

activity, whereas the phosphorylated Cx43 blocks such activity (14). Recent studies have shown that protein kinase C–mediated excessive phosphorylation of Cx43 may contribute to the reduction of GJIC activity (15) in aortic endothelial cells grown in high-glucose medium (16).

Although there is considerable information on expression of Cx37, Cx40, and Cx43 in endothelial cells from large vessels of bovine, rat (17,18), pig (13), and human (19), little is known about connexin expression or GJIC activity in microvascular endothelial cells. In this study, we investigated the effect of high glucose concentrations on GJIC activity in microvascular endothelial cells and determined whether changes in GJIC activity are associated with connexin gene expression.

RESEARCH DESIGN AND METHODS

Cell culture. Microvascular endothelial cells derived from rat epididymal fat pads ascertained positive for von Willebrand protein by immunofluorescence microscopy were used in this study (20). Cells were grown in Dulbecco's modified Eagle's medium containing 10% fetal bovine serum (Sigma, St. Louis, MO) and antibiotics. To determine the effect of high glucose on Cx43 expression and GJIC activity, these cells were grown in normal (5 mmol/l) or high (30 mmol/l) D-glucose medium for 9 days to confluency.

Gel electrophoresis and Western blot. Cells exposed to normal or high-glucose medium were washed with PBS and lysed in buffer containing 10 mmol/l Tris, pH 7.5 (Sigma), 1 mmol/l EDTA, and 0.1% Triton X-100 (Sigma). Cellular protein content in the cell extract was measured by bicinchoninic acid protein assay method (Pierce, Rockford, IL). After addition of an equal volume of 2× sample buffer and denaturation at 95°C for 5 min, the extracts (containing 30 μg protein) were electrophoresed at 260 V for 2 h. Molecular weight standards (Bio-Rad, Richmond, CA) were included in separate lanes in each gel. After electrophoresis, the proteins were transferred onto nitrocellulose membrane (Bio-Rad) according to the procedure of Towbin et al. (21) using a semidry apparatus with Towbin buffer system. Western blot analysis was performed to examine the steady-state levels of Cx37, Cx40, and Cx43 expression in these cells. The proteins transferred to the nitrocellulose membrane were detected with the Immun-Star Chemiluminescent Protein Detection System (Bio-Rad) and rabbit anti–mouse Cx37, Cx40 antiserum (Alpha Diagnostic, San Antonio, TX), and mouse anti–rat Cx43 antiserum (Chemicon, Temecula, CA). Briefly, the membrane was blocked with 5% nonfat dry milk for 1 h and incubated with mouse anti–rat Cx43 antibody solution (1:500) in 0.2% nonfat milk for 1 h. The blot was washed with Tris-buffered saline containing 0.1% Tween-20 and then incubated with antibody solution containing goat anti–mouse IgG antibody conjugated with alkaline phosphatase enzyme (Sigma) for 1 h. The membrane was washed as above, applied to the Immun-Star chemiluminescent substrate, and exposed to X-ray film (Fuji, Tokyo, Japan). The amounts of protein loaded in the gel lanes were confirmed through duplicate gels that were prepared simultaneously. A similar procedure was followed for detection of Cx37 and Cx40. For treatment of the samples with alkaline phosphatase (AP) to assess the phosphorylation of Cx43, the samples were, in part, preincubated with AP (10 U/ml calf intestine phosphatase; Boehringer Mannheim, Indianapolis, IN) for 20 min at 30°C and then subjected to Western blot analysis, as described above. Densitometric analysis of the luminescent signal was performed at nonsaturating exposures with a laser scanning densitometer.

Immunofluorescence microscopy. To study the distribution pattern and relative amounts of Cx43, immunofluorescence staining for Cx43 was performed on RME cells grown in normal or high-glucose medium. Briefly, cells grown to confluency were fixed in ice-cold methanol for 15 min, washed in PBS, and treated with 2% BSA for 15 min to block nonspecific antibody binding. The cells were then incubated overnight at 4°C in a moist chamber with a monoclonal mouse anti–rat Cx43 antibody (Chemicon) diluted 1:100 in PBS containing 2% BSA. After three PBS washes, the cells were incubated for 1 h with fluorescein isothiocyanate–conjugated goat anti-mouse IgG (Sigma) diluted 1:100 in PBS containing 2% BSA. After three PBS washes, coverslips were mounted in Slow-Fade (Molecular Probes, Eugene, OR). Negative control samples were processed in exactly the same way as those in the experimental groups except that the primary antibody was omitted. The cells were viewed and photographed using a confocal microscope (LSM510; Zeiss, Göttingen, Germany) equipped with LSM510 software (version 2.01; Zeiss). The punctate fluorescence counts were assessed at the site of contact between adjacent cells within a different and random area of 27 × 27 μm. Counts obtained from cells hybridized without primary antibody were used as background and subtracted from counts obtained from cells grown in normal or high-glucose medium.

Detection and quantitation of relative levels of Cx43 mRNA

RT-PCR. In each experiment, RNA from cells grown in normal medium was processed in parallel with RNA from cells grown in high-glucose medium. RT reactions were performed in 20 μl volume, with 1 μg RNA, 200 units of reverse transcriptase, 2.5 μmol/l random hexamers, 1 mmol/l of each dNTPs, 5 mmol/l $MgCl_2$, PCR buffer, and RNase inhibitor for 10 min at room temperature followed by 40 min at 42°C. At the end of RT, samples were heated to 95°C for 5 min, cooled on ice, and treated with RNase H (1 unit) for 15 min at 37°C. PCR was designed to measure the level of Cx43 expression relative to the expression of an endogenous internal standard gene, β-actin. To prevent quantitative inaccuracies deriving from competitive effects and different efficiency and ranges of amplification of the two cDNAs, the Cx43 and β-actin cDNAs generated in the same RT reaction were amplified in separate tubes containing increasing volumes of the RT reaction (1, 2, and 4 μl) to document amplification in the linear region for each cDNA. The primers used to amplify Cx43 (5′-GAATCCTGCTCCTGG-3′ and 5′-GATGCTGATGATGTAG-3′) and β-actin (5′-ATGGATGACGATATCGCT-3′ and 5′-ATCACAATGCCAGTGGTA-3′) were designed from the European Molecular Biology Laboratory (EMBL) sequences (accession no. NM 012567 for Cx43 and J00691 for β-actin). The specificity of the PCR was enhanced by using the "hot start" approach (22). The PCR containing the appropriate aliquot of RT material with primers, 0.2 μmol/l each, 2.5 U AmpliTaq DNA polymerase (Boehringer Mannheim), $MgCl_2$ (1.8 mmol/l), and PCR buffer in 50 μl volume was performed in a DNA thermal cycler (Hybaid, Middlesex, U.K.) using the following cycle conditions: denaturation for 1 min at 95°C, annealing for 1 min at 54°C, and extension for 2 min at 72°C. PCR was performed with 25 cycles for Cx43 and 27 cycles for β-actin.

Analysis and quantitation of PCR products. PCR products were always resolved on the same gel (1.0% agarose) containing 0.05 μl/ml GelStar (BMA, Rockland, ME) together with molecular weight markers (100-bp DNA ladder; Gibco, Grand Island, NY). The gel was photographed with Positive/Negative Instant Film (665; Polaroid, Cambridge, MA). Signal intensity was quantitated at nonsaturating exposure of the Polaroid film with a Zeineh soft laser scanning densitometer (Biomed Instruments, Chicago, IL). The densitometric values of the PCR products generated from increasing volumes of RT reaction were averaged to yield the Cx43 and β-actin signals for each sample (densitometric units per microliter of RT reaction).

Northern blot analysis. Total RNA was extracted from rat embryo cells grown in normal or high-glucose medium using RNAgents Total RNA Isolation System (Promega) following the manufacturer's instructions. Electrophoresis was performed with 10 μg RNA samples in 1% denaturing agarose gel containing 2.2 mol/l formaldehyde. The RNA was transferred onto a nylon membrane (Micron Separations, Westboro, MA) and hybridized to a biotin-labeled rat Cx43 cDNA and to a β-actin RNA probe (Kirkegaard & Perry Laboratories [KPL], Gaithersburg, MD). The biotin-labeled Cx43 probe was generated with Detector Random Primer DNA Biotinlyation kit (KPL) using biotin-N_4-dCTP. Prehybridization and hybridization were carried out at 42°C for Cx43 probe and at 65°C for β-actin probe. After hybridization, the membranes were washed and subjected to AP-Streptavidin and CDP-Star detection system using RNA Detector Northern Blotting Kit (KPL). Briefly, this chemiluminescent detection system relies on the use of AP, a reporter enzyme that catalyzes CDP-Star, a 1,2-dioxetane chemiluminescent substrate, during the last step of the detection system to produce luminescent signals. The chemiluminescent signal was then detected by exposing to Fuji X-ray film. Densitometry was performed at nonsaturating exposures. Statistical analysis was performed on the Cx43/β-actin ratios and recorded for the normal and high-glucose groups.

Cell-cell communication assay. We used the scrape-loading dye transfer (SLDT) technique (23, 24) to assess GJIC activity. Briefly, cells were grown in normal or high-glucose medium to confluency and rinsed three times with PBS containing 0.01% Ca^{2+} and 0.01% Mg^{2+} (Ca^{2+},Mg^{2+}-PBS). An aliquot of 1.5 ml PBS containing 0.05% Lucifer yellow CH (Molecular Probes) was added to the medium, and several scrapes (cuts) were made on the monolayer using a surgical scalpel. The cells were incubated for 3 min at room temperature in the dye solution and then rinsed three times with Ca^{2+},Mg^{2+}-PBS to remove any background fluorescence. The cells were then fixed with 1 ml of 4% formalin and photographed using a confocal microscope (LSM510). The dye-coupled cells on either side of the scrape line were counted in random areas to evaluate the GJIC activity in RME cells grown in normal or high-glucose medium.

Statistical analysis. Data are expressed as means ± SD or SE. Comparisons between groups were performed with Student's t test. A level of $P < 0.05$ was considered statistically significant.

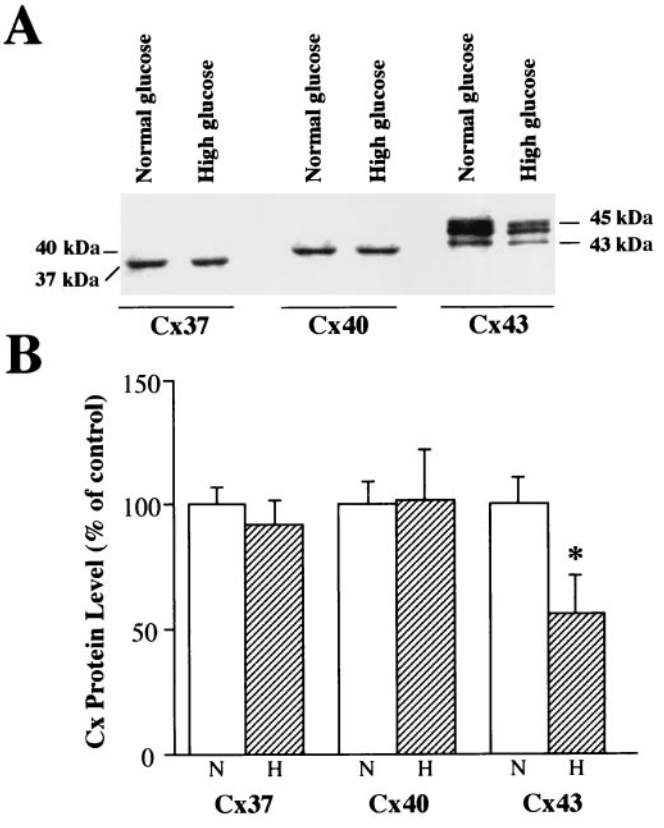

FIG. 1. *A*: Western blot analysis of Cx37, Cx40, and Cx43 protein levels in RME cells grown in normal or high-glucose medium. *B*: Cx43 protein levels are reduced in cells grown in high-glucose medium compared with cells grown in normal medium, whereas Cx37 and Cx40 protein levels are not altered by high glucose concentrations.

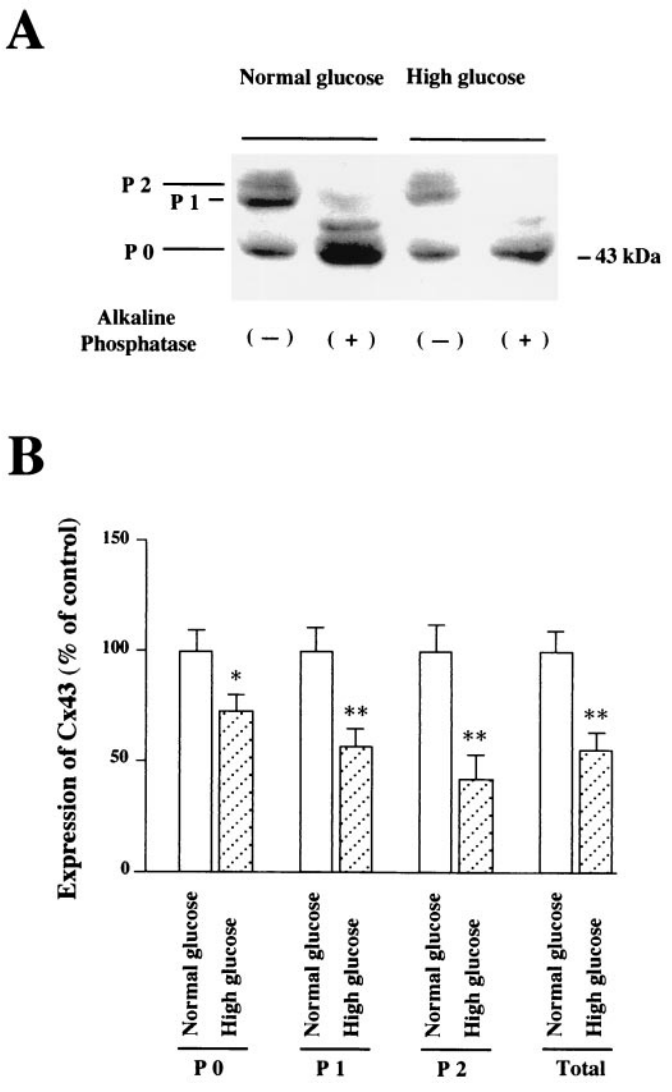

FIG. 2. Effect of high glucose on Cx43 protein levels and Cx43 phosphorylation pattern in RME cells. *A*: Western blot analysis of Cx43 protein levels in cells grown in normal medium (*lanes 1* and *2*) or high-glucose medium (*lanes 3* and *4*) for 9 days. Protein extracted from cells treated with (*lanes 2* and *4*) or without (*lanes 1* and *3*) AP. The positions of a 43-kDa molecular weight marker, nonphosphorylated (P0) and phosphorylated (P1 and P2) forms of Cx43 are indicated. This is a representative Western blot from six experiments. *B*: Analysis of the intensity of the bands corresponding to the indicated nonphosphorylated and phosphorylated forms of Cx43. Data are means ± SE and expressed as percent of control ($n = 5$). *$P < 0.05$, **$P < 0.01$.

RESULTS

Effect of high glucose concentration on connexin protein level and phosphorylation of Cx43. Rat microvascular endothelial cells grown in high-glucose medium for 9 days exhibited reduced Cx43 expression. Cx43 protein level was significantly reduced (55.6 ± 16% of control; $P = 0.003$, $n = 5$); however, there was no effect on the expression of Cx37 or Cx40 protein levels (92 ± 20% and 102 ± 11% of control, respectively) in cells grown in high-glucose medium (Fig. 1). Western blot analyses and AP treatment revealed that Cx43 protein existed in multiphosphorylated forms, consisting of a nonphosphorylated form (P0) and two phosphorylated forms (P1 and P2) ranging in size between 43 and 45 kDa in cultured RME cells (Fig. 2*A*). AP treatment resulted in an increase in the density of the P0 form at the expense of the other two forms, P1 and P2 (Fig. 2*A*). In cells grown in high-glucose medium, all three forms showed a significant decrease in the intensity of the bands: P0, 73 ± 15% of control ($P = 0.04$); P1, 57 ± 16% of control ($P = 0.008$); and P2, 42 ± 22% of control ($P = 0.006$) (Fig. 2*A* and *B*). Overall, Cx43 (P0 + P1 + P2) protein level was reduced by the high-glucose conditions (55.6 ± 16% of control; $P = 0.003$, $n = 5$) (Fig. 2*A* and *B*).

Effect of high glucose concentrations on Cx43 localization and cell-cell contact. The distribution and relative quantity of Cx43 expression in RME cells were determined using immunofluorescence microscopy. Cx43 localization could be ascertained from punctate "dot-like" (plaques) pattern at the sites of contact between adjacent cells (Fig. 3*A* and *B*). The intensity of Cx43 immunofluorescence was less in cells grown in high-glucose medium compared with cells grown in normal medium, and the number of plaques was less in cells grown in high-glucose medium (Fig. 3*A* and *B*). A semiquantitative analysis of Cx43 at cell-cell contacts, based on counts from plaques within defined areas, yielded a score of 54 ± 5 for cells grown in normal medium and 34 ± 3 for cells grown in high-glucose medium, indicating reduced Cx43 junctional protein at the cell membrane of cells grown in high-glucose medium (63% of control; $P < 0.01$, $n = 5$) (Fig. 3*C*).

Effect of high glucose concentrations on Cx43 mRNA levels. Cx43 mRNA levels determined by RT-PCR or Northern blot analysis in RME cells grown in high-glucose medium indicated significant downregulation compared

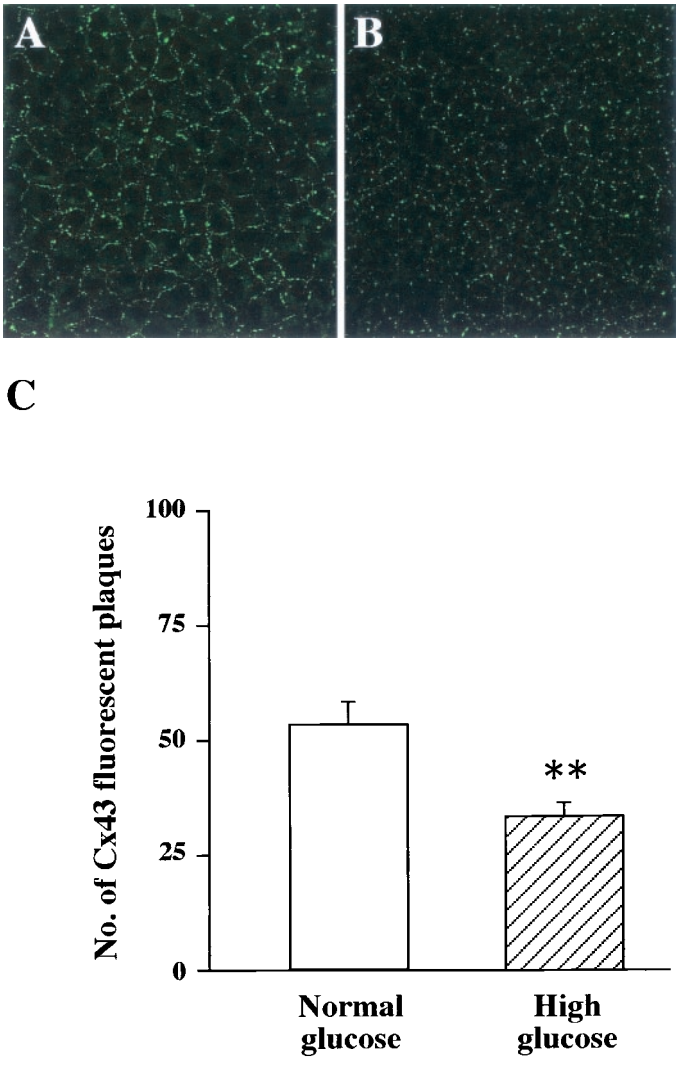

FIG. 3. Effect of high glucose on Cx43 immunoreactivity in RME cells. Representative photomicrographs of cells grown in normal medium (*A*) and cells grown in high-glucose medium (*B*). Note the "dot-like" punctate fluorescence pattern at the site of contact between adjacent cells. Original magnification ×350. *C*: Counts from punctate fluorescence in cells grown in normal or high-glucose medium. Data are means ± SD (n = 5). **P < 0.01.

with cells grown in normal medium (Fig. 4). Figure 4*A* shows Cx43 and β-actin RT-PCR products after gel electrophoresis in which high-glucose conditions reduced Cx43 mRNA levels (68 ± 13% of control; $P = 0.019$, $n = 5$). The β-actin mRNA level used as an internal control showed no change (98% of control). The band intensity of the RT-PCR products increased linearly with the increasing amount of RT reaction (1, 2, and 4 μl) for both Cx43 and β-actin, indicating that comparisons between normal and high-glucose products were made within the exponential phase of the reaction (Fig. 4*A* and *B*). Figure 4*B* represents Cx43 mRNA levels generated from all volumes of RT reactions. Figure 4*C* shows relative levels of Cx43 and β-actin mRNA on a Northern blot. Cx43 levels were clearly reduced in cells grown in high-glucose medium compared with normal medium (58 ± 12% of control; $P = 0.01$), whereas the β-actin mRNA level was unchanged (Fig. 4*C* and *D*).

Effect of high glucose concentrations on GJIC activity in RME cells. To understand the association between reduced Cx43 expression and GJIC activity, we assessed the ability of RME cells to transfer Lucifer yellow through gap junctions using the SLDT technique in corresponding cultures of cells with reduced Cx43 expression. The total number of dye-coupled cells on either side of the scrape line was clearly less in high-glucose medium compared with normal medium (Fig. 5*A* and *B*). When the number of dye-coupled cell layers were counted from the edge of the scrape, reduced dye transfer was evident; only three to four layers in high-glucose medium were positive compared with seven in normal medium (3.9 ± 0.6 vs. 6.5 ± 1.0; $P < 0.01$, $n = 5$), i.e., 60% of control (Fig. 5*A*, *B*, and *C*). The reduced GJIC activity also showed a striking correlation with the downregulation of Cx43 expression in high-glucose cells ($r = 0.9$).

DISCUSSION

To evaluate whether high glucose levels affected endothelial connexin expression and GJIC activity, we assessed mRNA and protein levels and, as a functional assay, examined dye transfer after scrape load in RME cells exposed to high-glucose medium. Of the three endothelial-specific connexins we studied, we found the expression of only Cx43 to be altered. Whereas Cx37 and Cx40 expression showed no change in RME cells grown in high-glucose medium, Cx43 expression was significantly reduced at both the mRNA and protein levels. In addition, immunofluorescence microscopy showed reduced numbers of Cx43 gap junctions at the site of contact between adjacent cells grown in high-glucose medium.

Alkaline phosphatase treatment resulted in almost complete removal of the P1 and P2 bands, with corresponding increase in intensity of the P0 band, suggesting that the P1 and P2 bands are the two forms of phosphorylated connexin, and that the P0 band is the unphosphorylated form of connexin protein. High-glucose conditions in our experiments showed overall reduction in expression of all three forms of Cx43. Consistent with these results, Granot and Dekel (25), using rat ovarian cells, also reported three forms of Cx43 with molecular weights between 43 and 45 kDa. When we examined RME cells grown in high-glucose medium with the SLDT assay in which Lucifer yellow transfer was measured after scrape-load, we found a significant reduction in GJIC activity compared with cells grown in normal medium. This reduced GJIC activity showed a strong correlation with the reduced Cx43 expression in high-glucose cells ($r = 0.9$). Similar to our results, Kuroki et al. (15) observed inhibition of GJIC activity in cultured vascular smooth muscle cells grown in high-glucose medium using the fluorescent dye transfer method. Taken together, these results indicate that Cx43 exists in multiphosphorylated forms and that the expression of both the nonphosphorylated and phosphorylated forms are downregulated in RME cells, with corresponding reduction in GJIC activity, under high glucose concentration.

In this study, we observed that high glucose impairs not only connexin expression in microvascular endothelial cells but also its functional activity. A link between reduced GJIC activity and reduced connexin gene expression has been previously reported in rat ovarian cells exposed to luteinizing hormone, which resulted in de-

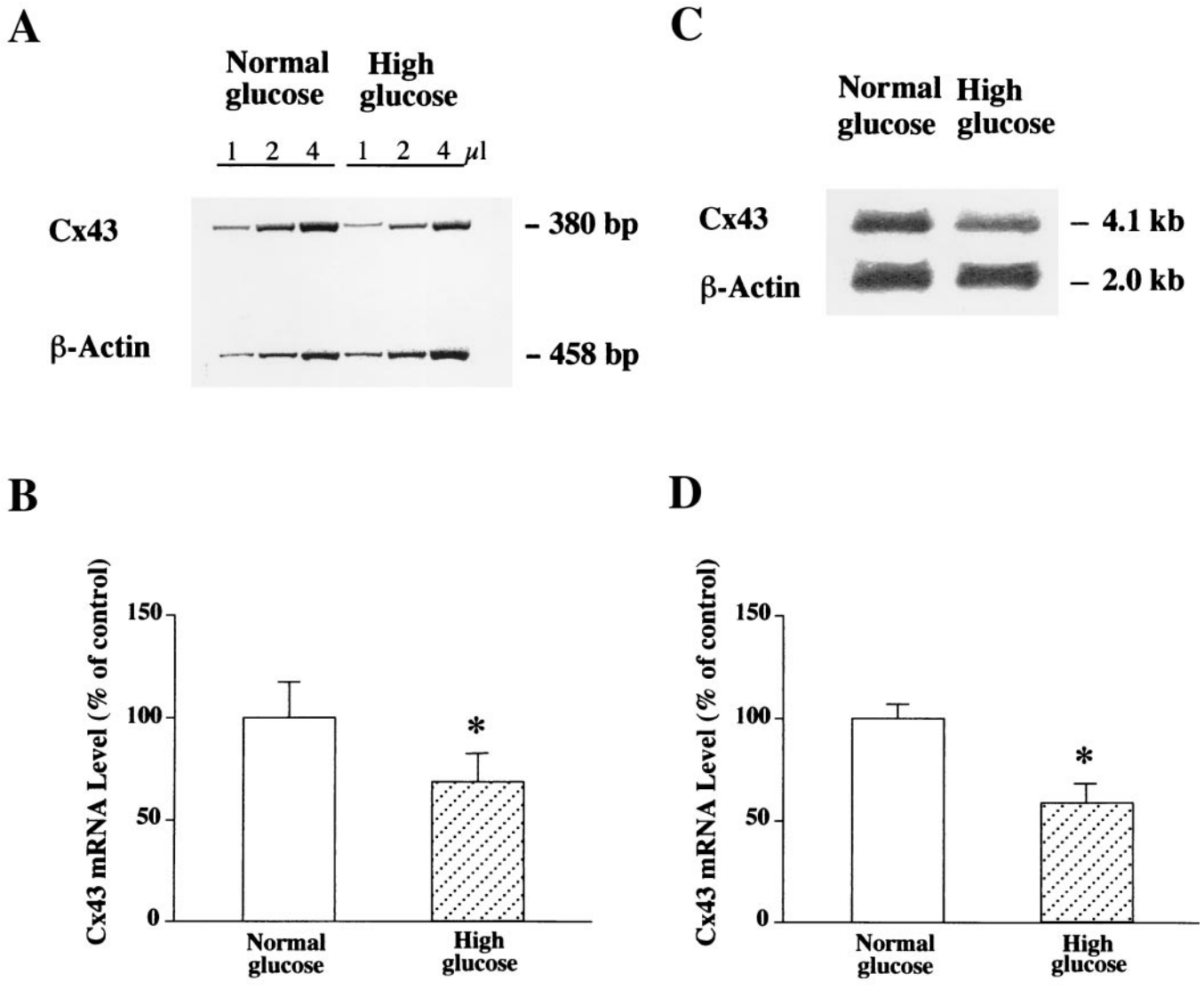

FIG. 4. Effect of high glucose on Cx43 mRNA levels in RME cells. *A*: RT-PCR analysis of Cx43 mRNA levels in cells exposed to normal or high-glucose medium: PCR amplification products for Cx43 and β-actin as detected on GelStar-stained agarose gel with 1, 2, and 4 μl reverse-transcribed cDNA. PCR with Cx43 primer pair generated a single 380-bp product; PCR with β-actin primer pair generated a single 458-bp product. *B*: Cx43 mRNA levels determined by RT-PCR in cells grown in normal or high-glucose medium. *C*: Northern blot analysis of Cx43 mRNA levels in cells grown in normal or high-glucose medium. *D*: Cx43 mRNA levels determined by Northern blot analysis in cells grown in normal or high-glucose medium. Data are means ± SD and are expressed as percent of control after normalizing to β-actin mRNA levels ($n = 5$). *$P < 0.05$.

creased Cx43 mRNA levels by 45%, with subsequent reduction in GJIC activity (25). Studies have shown Cx43 to interact with the NH_2-terminal domain of ZO-1, a component of the tight junction in endothelial cells (26). Because ZO-1 expression is reduced under high-glucose conditions (27), it is possible that the effect of high glucose on GJIC activity may be mediated via other junction protein components. Our findings indicate that reduced GJIC activity in RME cells exposed to high glucose is at least in part due to inhibition of Cx43 gene expression.

Reduced GJIC could contribute to diabetic vasculopathy by a number of mechanisms. Inhibition of GJIC activity induced by high glucose concentrations may impair diffusible transport of small molecules such as calcium ions necessary for cell proliferation and maintenance of cellular homeostasis. GJIC may also play a role in cell proliferation, cell differentiation, and apoptosis (28), a process known to occur in cultured endothelial cells and pericytes (29) and the loss of retinal capillary endothelial cells and pericytes in diabetic retinopathy (30–32). Reduced GJIC in retinal endothelial cells could affect other retinal cells: retinal astrocytes, Muller cells, and pericytes. These cells, together with the endothelial cells, maintain homeostasis of the BRB. Studies have shown that the surface retinal vessels of all calibers are in contact with the processes of astrocytes (33), and extensive gap junctions composed primarily of Cx43 (34) characterize these astrocytes. Dye transfer assay has revealed that rat retinal astrocytes are coupled to each other and to Muller cells (35). Because Cx43 reactivity has been detected at the interface of astrocytes and endothelial cells in co-cultures (36), reduced Cx43 expression by high glucose may lead to reduced GJIC between astrocytes and endothelial cells and between astrocytes and Muller cells. Because pericytes and endothelial cells communicate via gap junctions (37), express Cx43 mRNA (4), and have a high frequency

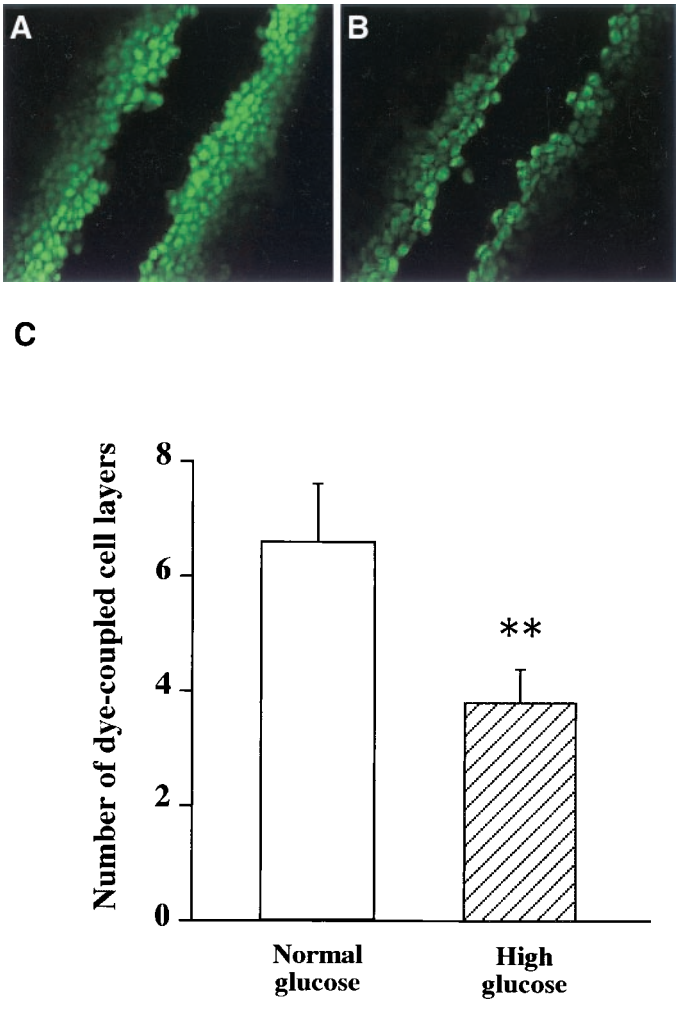

FIG. 5. Analysis of GJIC activity in RME cells using SLDT technique: transfer of Lucifer yellow into contiguous cells detected after scrape-loading. Lucifer yellow was detected in six to eight layers on either side of the scrape line in cells grown in normal medium (*A*) compared with three to five layers in cells grown in high-glucose medium (*B*), indicating reduced GJIC activity in cells grown in high-glucose medium. Original magnification ×210. *C*: Counts from dye-coupled cell layers in normal or high-glucose medium. Data are means ± SD ($n = 5$). **$P < 0.01$.

of junctional contact between endothelial cells and pericytes (4), it is likely that high glucose–induced reduction of Cx43 expression could impair GJIC and contribute to retinal capillary cell death.

The cause of BRB breakdown in diabetes remains controversial, with some investigators reporting that BRB breakdown is mediated by altered membrane permeability and increased vesicle formation without tight junction alteration (38,39) and others that junction protein expression is altered in diabetes (40). Findings from this study indicate that high glucose levels reduce GJIC activity in microvascular endothelial cells by inhibiting Cx43 gene expression. Further studies are necessary to clarify the role of altered GJIC activity in the pathogenesis of diabetic retinopathy.

ACKNOWLEDGMENTS

Work on connexin gene expression was supported in part by grants from the American Diabetes Association, Chartrand Foundation, the Macula Foundation, MA Lions Eye Research Foundation, the National Institutes of Health, and Research to Prevent Blindness.

REFERENCES

1. Beyer EC: Gap junctions. *Int Rev Cytol* 1–37, 1993
2. Johansson K, Bruun A, Ehinger B: Gap junction protein connexin43 is heterogeneously expressed among glial cells in the adult rabbit retina. *J Comp Neurol* 407:395–403, 1999
3. Janssen-Bienhold U, Dermietzel R, Weiler R: Distribution of connexin43 immunoreactivity in the retinas of different vertebrates. *J Comp Neurol* 396:310–321, 1998
4. Larson DM, Haudenschild CC, Beyer EC: Gap junction messenger RNA expression by vascular wall cells. *Circ Res* 66:1074–1080, 1990
5. Little TL, Beyer EC, Duling BR: Connexin 43 and connexin 40 gap junctional proteins are present in arteriolar smooth muscle and endothelium in vivo. *Am J Physiol* 268:H729–H739, 1995
6. Frank RN, Turczyn TJ, Das A: Pericyte coverage of retinal and cerebral capillaries. *Invest Ophthalmol Vis Sci* 31:999–1007, 1990
7. Yamagishi S, Hsu CC, Kobayashi K, Yamamoto H: Endothelin 1 mediates endothelial cell-dependent proliferation of vascular pericytes. *Biochem Biophys Res Commun* 31:840–846, 1993
8. Do carmo A, Ramos P, Reis A, Proenca R, Cunha-vaz JG: Breakdown of the inner and outer blood retinal barrier in streptozotocin-induced diabetes. *Exp Eye Res* 67:569–575, 1998
9. Dejana E, Corada M, Lampugnani MG: Endothelial cell-to-cell junctions. *Faseb J* 9:910–918, 1995
10. Himpens B, Stalmans P, Gomez P, Malfait M, Vereecke J: Intra- and intercellular Ca^{2+} signaling in retinal pigment epithelial cells during mechanical stimulation. *Faseb J* 13:S63–S68, 1999
11. Gao Y, Spray DC: Structural changes in lenses of mice lacking the gap junction protein connexin43. *Invest Ophthalmol Vis Sci* 39:1198–1209, 1998
12. Yeh HI, Rothery S, Dupont E, Coppen SR, Severs NJ: Individual gap junction plaques contain multiple connexins in arterial endothelium. *Circ Res* 83:1248–1263, 1998
13. van KM, Jongsma HJ: Distribution of connexin37, connexin40 and connexin43 in the aorta and coronary artery of several mammals. *Histochem Cell Biol* 112:479–486, 1999
14. Hossain MZ, Ao P, Boynton AL: Platelet-derived growth factor-induced disruption of gap junctional communication and phosphorylation of connexin43 involves protein kinase C and mitogen-activated protein kinase. *J Cell Physiol* 176:332–341, 1998
15. Kuroki T, Inoguchi T, Umeda F, Ueda F, Nawata H: High glucose induces alteration of gap junction permeability and phosphorylation of connexin-43 in cultured aortic smooth muscle cells. *Diabetes* 47:931–936, 1998
16. Inoguchi T, Ueda F, Umeda F, Yamashita T, Nawata H: Inhibition of intercellular communication via gap junction in cultured aortic endothelial cells by elevated glucose and phorbol ester. *Biochem Biophys Res Commun* 208:492–497, 1995
17. Yeh HI, Chang HM, Lu WW, Lee YN, Ko YS, Severs NJ, Tsai CH: Age-related alteration of gap junction distribution and connexin expression in rat aortic endothelium. *J Histochem Cytochem* 48:1377–1389, 2000
18. Yeh HI, Lai YJ, Chang HM, Ko YS, Severs NJ, Tsai CH: Multiple connexin expression in regenerating arterial endothelial gap junctions. *Arterioscler Thromb Vasc Biol* 20:1753–1762, 2000
19. van Rijen HV, van Kempen MJ, Postma S, Jongsma HJ: Tumour necrosis factor alpha alters the expression of connexin43, connexin40, and connexin37 in human umbilical vein endothelial cells. *Cytokine* 10:258–264, 1998
20. Roy S, Roth T: Proliferative effect of high glucose is modulated by antisense oligonucleotides against fibronectin in rat endothelial cells. *Diabetologia* 40:1011–1017, 1997
21. Towbin H, Staehelin T, Gordon J: Electrophoretic transfer of proteins from polyacrylamide gels to nitrocellulose sheets: procedure and some applications. *Proc Natl Acad Sci U S A* 76:4350–4354, 1979
22. Erlich HA, Gelfand D, Sninsky JJ: Recent advances in the polymerase chain reaction. *Science* 252:1643–1651, 1991
23. el-Fouly MH, Trosko JE, Chang CC: Scrape-loading and dye transfer: a rapid and simple technique to study gap junctional intercellular communication. *Exp Cell Res* 168:422–430, 1987
24. DeoCampo ND, Wilson MR, Trosko JE: Cooperation of bcl-2 and myc in the neoplastic transformation of normal rat liver epithelial cells is related to the down-regulation of gap junction-mediated intercellular communication. *Carcinogenesis* 21:1501–1506, 2000
25. Granot I, Dekel N: Phosphorylation and expression of connexin-43 ovarian

gap junction protein are regulated by luteinizing hormone. *J Biol Chem* 269:30502–30509, 1994
26. Toyofuku T, Yabuki M, Otsu K, Kuzuya T, Hori M, Tada M: Direct association of the gap junction protein connexin-43 with ZO-1 in cardiac myocytes. *J Biol Chem* 273:12725–12731, 1998
27. Gardner TW: Histamine, ZO-1 and increased blood-retinal barrier permeability in diabetic retinopathy. *Trans Am Ophthalmol Soc* 93:583–621, 1995
28. Trosko JE, Chang CC, Wilson MR, Upham B, Hayashi T, Wade M: Gap junctions and the regulation of cellular functions of stem cells during development and differentiation. *Methods* 20:245–264, 2000
29. Baumgartner-Parzer SM, Wagner L, Pettermann M, Grillari J, Gessl A, Waldhausl W: High-glucose–triggered apoptosis in cultured endothelial cells. *Diabetes* 44:1323–1327, 1995
30. Li W, Liu X, Yanoff M, Cohen S, Ye X: Cultured retinal capillary pericytes die by apoptosis after an abrupt fluctuation from high to low glucose levels: a comparative study with retinal capillary endothelial cells. *Diabetologia* 39:537–547, 1996
31. Roy S, Angeles C, Lorenzi M: Accelerated death of pericytes after longterm exposure to high glucose in vitro (Abstract). *Diabetes* 47:A140, 1998
32. Mizutani M, Kern TS, Lorenzi M: Accelerated death of retinal microvascular cells in human and experimental diabetic retinopathy. *J Clin Invest* 97:2883–2890, 1996
33. Zahs KR, Wu T: Confocal microscopic study of glial-vascular relationships in the retinas of pigmented rats. *J Comp Neurol* 429:253–269, 2001
34. Naus CC, Bani-Yaghoub M, Rushlow W, Bechberger JF: Consequences of impaired gap junctional communication in glial cells. *Adv Exp Med Biol* 468:373–381, 1999
35. Zahs KR, Newman EA: Asymmetric gap junctional coupling between glial cells in the rat retina. *Glia* 20:10–22, 1997
36. Braet K, Paemeleire K, D'Herde K, Sanderson MJ, Leybaert L: Astrocyte-endothelial cell calcium signals conveyed by two signalling pathways. *Eur J Neurosci* 13:79–91, 2001
37. Hirschi KK, D'Amore PA: Pericytes in the microvasculature. *Cardiovasc Res* 32:687–698, 1996
38. Caldwell RB, Slapnick SM, McLaughlin BJ: Lanthanum and freeze-fracture studies of retinal pigment epithelial cell junctions in the streptozotocin diabetic rat. *Curr Eye Res* 4:215–227, 1985
39. Caldwell RB, Slapnick SM: Freeze-fracture and lanthanum studies of the retinal microvasculature in diabetic rats. *Invest Ophthalmol Vis Sci* 33:1610–1619, 1992
40. Antonetti DA, Barber AJ, Khin S, Lieth E, Tarbell JM, Gardner TW: Vascular permeability in experimental diabetes is associated with reduced endothelial occludin content: vascular endothelial growth factor decreases occludin in retinal endothelial cells. Penn State Retina Research Group. *Diabetes* 47:1953–1959, 1998